

Heavy vector-like quark with charge $5/3$ at the LHC

Giacomo Cacciapaglia,^a Aldo Deandrea,^a Luca Panizzi,^b Stéphane Perries^a and Viola Sordini^a

^a*Université de Lyon, France; Université Lyon 1, CNRS/IN2P3, UMR5822 IPNL, F-69622 Villeurbanne Cedex, France*

^b*School of Physics and Astronomy, University of Southampton, Highfield, Southampton SO17 1BJ, UK.*

E-mail: g.cacciapaglia@ipnl.in2p3.fr, deandrea@ipnl.in2p3.fr,
s.perries@ipnl.in2p3.fr, sordini@ipnl.in2p3.fr, l.panizzi@soton.ac.uk

ABSTRACT: We study the phenomenology at the Large Hadron Collider of an exotic vector-like quark with charge $+5/3$. We relax the assumption of a 100% branching into Wt and allow for an arbitrary rate into W plus light quarks, thus covering all possible scenarios. Sizeable decays into light quarks can be achieved, for instance, in a model where the $X_{5/3}$ quark is embedded in a doublet with hypercharge $7/6$, which also contains a t' quark. We study the bounds on the parameter space of this model, and perform a detailed simulation of the $X_{5/3}$ pair production and decays. We show that the final state with $WtWq$, where $q = u$ or c , contributes to the same sign dilepton searches, and that the reach can be improved with alternative cuts optimised on such final state.

KEYWORDS: heavy exotic vector-like quarks, heavy quark production and decays

Contents

1	Introduction	1
2	Mixing parameters in the non-SM doublet model	3
2.1	$X_{5/3}$ production and decay	6
2.2	Present bounds	7
3	Simulation Details	9
3.1	Signal	9
3.2	Identification of SM backgrounds	10
3.3	Detector simulation	10
4	Analysis and results	11
4.1	Mass limit for fixed BRs	12
4.2	Analysis with $\text{BR}(X_{5/3} \rightarrow tW)$ as a free parameter	14
5	Conclusions	15

Contents

1 Introduction

The top quark certainly plays a special role in the Standard Model (SM), because it is the only fermion with a mass close to the electroweak scale, thus coupling strongly with the Higgs sector. Any model of new physics which attempts to solve the hierarchy problem, or that aims at modifying the properties of the Higgs boson, will likely predict the presence of heavy partners of the top. Among these new states, vector-like quarks occupy a special place for their role in model building, as they are often predicted by models based on new symmetries: in extra dimensional models, for example, they appear as Kaluza-Klein recurrences of the standard model quarks; in little Higgs type models they ensure the cancellation of the top Yukawa divergent loop [1]; in models where a new strongly-coupled sector is responsible for the breaking of the electroweak (EW) symmetry they emerge as part of the composite sector [2] or are predicted when a custodial symmetry is introduced to protect the coupling $Zb\bar{b}$ from large deviations [3]. The presence of TeV scale vector-like quarks is also an interesting possibility for their effect on the Higgs properties: for instance, supersymmetric models with vector-like quarks can ease the MSSM tension in the Higgs mass whose value is lifted from the tree level prediction $m_H \sim m_Z$ via loop contributions [4–6]; they have also been proposed as a solution [7–9] for the apparent excess in the $H \rightarrow \gamma\gamma$ rate observed by both CMS and ATLAS (for a general discussion of

the effect of new particles to the $H \rightarrow \gamma\gamma$ decay mode see [10, 11]). Vector-like quarks are also phenomenologically interesting as, depending on the choice of their quantum numbers, they may be much less constrained than a fourth family of standard model like quarks. By simply requiring the presence of a Yukawa-type coupling with the standard quarks, the allowed representations can contain both a top and bottom partner (t' and b'), but also two exotic quarks with charges $+\frac{5}{3}$ ($X_{5/3}$) and $-\frac{4}{3}$ ($Y_{-4/3}$)¹. In [12] a complete list of the possible representations is presented, including the relevant bounds from precisely measured quantities in the Standard Model (SM). For earlier bounds see for example [13, 14]. However the most competitive bounds will come in the short term from direct searches at the Large Hadron Collider (LHC). The LHC is indeed collecting data that allow to test this sector quite precisely up to a few hundred GeV, and many bounds have already been published based on the 2011 dataset at 7 TeV, while the 2012 run at 8 TeV awaits to be analysed. A review of the 2011 bounds can be found in [15]. However precise bounds crucially depend on the decay modes of the new states. In the experimental searches, the simplified assumption is often to consider 100% branching ratio in a single channel, and pair production via QCD interactions, which is independent on the charge and electroweak couplings of the new quark. However, no realistic case corresponds to this simplified assumption, and the bounds often cannot be translated in a straightforward manner to more realistic cases. In fact, the presence of various decay modes means that channels with mixed decays will also contribute to the signal region with an unknown experimental efficiency: a simple rescaling of the cross section with the branching ratios, therefore, is not sufficient to extract a reliable bound. Furthermore, typical cross-sections for single production of heavy vector-like quarks can become competitive with QCD pair production at high mass, even if they are model dependent. The exclusion limits from the 2011 data already fall in the mass region where both production channels are fairly large and may give comparable contribution to the signal.

Vector-like quarks have recently been the subject of wide interest as they may be the first hint of physics beyond the standard model to be seen at the LHC (for a general review see for example [15, 16]). Heavy vector-like quarks typically decay to SM quarks plus W and/or Z and Higgs bosons. Several decay modes of the t' and b' have been considered both by experimental searches and phenomenological studies, and a dedicated search for the exotic one $X_{5/3}$ is available from CMS [17]. In this paper we will focus in detail on the production and decays of such a state with electric charge 5/3, which is motivated, for example, by a custodial symmetry in models of composite Higgs [3]. It can only interact with SM up-type quarks through charged currents, while decays to a t' are only allowed for large mass splitting. Due to the exotic charge, its main distinctive decay mode is $X_{5/3} \rightarrow W^+ t \rightarrow W^+ W^+ b$, which can give rise to two same-sign leptons [18] via the W leptonic decays. This peculiar state was for example used in composite Higgs models searches [19, 20]. The same sign dilepton signature can also arise from the same final state with 4 W 's and 2 b 's which is also produced in the case of a b' quark decaying into

¹More exotic charges, like $+8/3$ and $-7/3$, can be obtained from larger $SU(2)$ representations when more than one vector-like quark are included.

$b' \rightarrow W^- t \rightarrow W^- W^+ b$, therefore, for example, the bound on the b' mass in [21, 22] can be directly translated into a bound on the $X_{5/3}$ mass because the experimental efficiencies in the two cases are very similar [23]. Both phenomenological studies and the dedicated CMS search consider 100% branching ratio into the top and pair production, while, in realistic set-ups, mixing with light fermions c and u can allow decays into W and a light jet. Such mixing is tightly bound by flavour observables, however depending on the case, the bounds can be fairly mild [24] and the branching ratio into light quarks can be competitive with the top one. Furthermore, the decay into light quarks may imply the presence of sizeable single $X_{5/3}$ production mediated by the same coupling with the W boson. On general ground, therefore, one cannot ignore the possibility of a sizeable coupling to light quarks. In light of this observation, in this paper we propose a more detailed study, where we consider pair production of the $X_{5/3}$ quark with more complete and realistic decay modes, allowing for decays into light quarks. The channel where both $X_{5/3}$ decay into W jet can be constrained by a search for heavy quarks decaying into Wq , with q being any light quark [25]. In this paper we do not consider single production of the $X_{5/3}$ state because it is a more model-dependent channel as it depends on the precise value of the mixing. We therefore postpone the single production analysis to a dedicated study, where we shall also address the matching procedure for the inclusion of QCD radiation, which is well under control only in the pair production case at present.

The results of our study can be applied to any model containing an exotic $X_{5/3}$ quark, as the only relevant parameters are the mass of the quark (which determines the pair production cross section) and the branching ratio into light quarks. However, to be more concrete and without loss of generality, our simulation is based on a model where the $X_{5/3}$ is embedded in a non-SM doublet with hypercharge $7/6$, which also contains a t' [24].

2 Mixing parameters in the non-SM doublet model

The phenomenology of the $X_{5/3}$ quark in the pair production channel can be fully characterised in terms of two free parameters:

- the mass M_X , which will determine the QCD production cross section;
- the branching ratio into tops, $BR(X_{5/3} \rightarrow W^+ t) = b$.

The branching into light quarks is therefore given by

$$BR(X_{5/3} \rightarrow W^+ u, W^+ c) = 1 - BR(X_{5/3} \rightarrow W^+ t) = 1 - b.$$

We are assuming here that $X_{5/3}$ cannot decay into $W^+ t'$ because such mode is not kinematically accessible. This assumption is quite general because in any reasonable model the splitting between the $X_{5/3}$ and t' belonging to the same $SU(2)$ multiplet can only be generated by Yukawa-type interactions via the Higgs vacuum expectation value (VEV), and such contribution is limited in size.

Without loss of generality, we will base our simulations on a specific simple model containing a vector-like quark which is an $SU(2)$ doublet with hypercharge $7/6$ (corresponding

to a shift of one hypercharge unit with respect to SM quark doublets). Such a doublet also contains a top partner t' which is studied in the literature (see for example [24] and references therein) due to its mixing with SM up-type quarks. The mass eigenstates are therefore:

$$\begin{pmatrix} u \\ d \end{pmatrix} \begin{pmatrix} c \\ s \end{pmatrix} \begin{pmatrix} t \\ b \end{pmatrix} \begin{pmatrix} X_{5/3} \\ t' \end{pmatrix} \quad (2.1)$$

In general, the t' mixes with all up-type quarks, and details of the mixing matrices for the general case of mixing with all three standard model families can be found for example in [24]. In this section we will simply recall the results relevant for our discussion of the $X_{5/3}$ phenomenology.

If the SM Higgs sector is not extended by the introduction of new scalars, the new doublet can only couple with the Higgs and the SM right-handed up-type singlets. The new Yukawa couplings generates a mixing in the up sector, with the three lighter mass eigenstates identified with the SM quarks. Denoting by u_R^i and u_L^i the SM singlets and up component of the doublets, and by $(X, U)^T$ the new doublet, the resulting mass terms are as follows (in the basis where the SM Yukawa couplings y_u are diagonal):

$$\mathcal{L}_{\text{mass}} = - \sum_{i=1}^3 \frac{y_u^i v}{\sqrt{2}} \bar{u}_L^i u_R^i - \sum_{i=1}^3 x_i \bar{U}_L u_R^i - M \bar{U}_L U_R - M \bar{X}_L X_R + h.c., \quad (2.2)$$

where $v \sim 246$ GeV is the Higgs VEV, y_u^i are the diagonal SM up Yukawas, M is the vector-like mass (also equal to the mass of $X_{5/3}$, $M_X = M$) and x_i encode the mixing generated by the Higgs VEV ($x_i = \frac{\lambda^i v}{\sqrt{2}}$, where λ^i are the new exotic Yukawa couplings). In the down sector, only the SM Yukawa matrix remains. We can first diagonalise the mass matrix for top and t' , thus neglecting the mixing with the light quarks:

$$\begin{pmatrix} \cos \theta_u^L & -\sin \theta_u^L \\ \sin \theta_u^L & \cos \theta_u^L \end{pmatrix} \begin{pmatrix} \frac{y_t v}{\sqrt{2}} & 0 \\ x_3 & M \end{pmatrix} \begin{pmatrix} \cos \theta_u^R & \sin \theta_u^R \\ -\sin \theta_u^R & \cos \theta_u^R \end{pmatrix} = \begin{pmatrix} m_t & 0 \\ 0 & m_{t'} \end{pmatrix}; \quad (2.3)$$

where:

$$\sin \theta_u^R = \frac{M x_3}{\sqrt{(M^2 - m_t^2)^2 + M^2 |x_3|^2}}, \quad \sin \theta_u^L = \frac{m_t}{M} \sin \theta_u^R. \quad (2.4)$$

Note that the mixing angle for left-handed components θ_L is typically smaller than the right-handed one θ_R , being suppressed by the mass of the top over the heavy mass M (which is typically larger). This property is still valid in the case of mixing with three flavours, with the left-handed mixing terms proportional to the light quark masses, while the right-handed ones are proportional to the Yukawa masses x_i . The mixing matrices are replaced by 4×4 unitary matrices V_L and V_R , acting respectively on the left- and right-handed components. The mass of t' is given by

$$m_{t'}^2 = M^2 \left(1 + \frac{|x_3|^2}{M^2 - m_t^2} \right) \left(1 + \frac{(|x_1|^2 + |x_2|^2) \cos^2 \theta_R}{M^2} + \dots \right), \quad (2.5)$$

$D_0-\bar{D}_0$ mixing	$ V_R^{41} V_R^{42} < 3.2 \times 10^{-4}$
APV in Cesium	$ V_R^{41} < 7.8 \times 10^{-2}$
LEP1, charm couplings	$ V_R^{42} < 0.2$
CMS: $t \rightarrow Zc, Zu$	$ V_R^{43} \sqrt{ V_R^{41} ^2 + V_R^{42} ^2} < 0.07 V_{tb} $

Table 1. Bounds on $|V_R^{41}|$ and $|V_R^{42}|$ from [24], and updated with the results in [26] for the top decays.

where we have kept the leading terms in x_1, x_2 and the light quark masses. From this formula it is clear that the presence of the new Yukawas always increases the t' mass so that $m_{t'} > M = M_X$, and that the splitting is typically small being suppressed by the vector-like mass M . In this model, therefore, the decay mode $X_{5/3} \rightarrow W^+ t'$ is absent, and we can expect this conclusion to hold in general because of the small splitting between the two masses.

The couplings of $X_{5/3}$ with top, charm and up are generated by the coupling with its SU(2) partner U , which mixes with the SM up quarks. The couplings with the mass eigenstates read:

$$\begin{aligned} \mathcal{L}_X = & i \frac{g}{\sqrt{2}} W_\mu^+ \bar{X}_R \gamma^\mu (V_R^{44} t'_R + V_R^{43} t_R + V_R^{42} c_R + V_R^{41} u_R) + \\ & i \frac{g}{\sqrt{2}} W_\mu^+ \bar{X}_L \gamma^\mu (V_L^{44} t'_L + V_L^{43} t_L + V_L^{42} c_L + V_L^{41} u_L) + h.c., \end{aligned} \quad (2.6)$$

where the relevant matrix elements are related to the new Yukawa couplings by:

$$\begin{aligned} V_R^{41} &= -\frac{x_1}{M}, & V_R^{42} &= -\frac{x_2}{M}, & V_R^{43} &= -\sin \theta_R, & V_R^{44} &= \cos \theta_R; \\ V_L^{41} &= -\frac{m_u x_1}{M^2}, & V_L^{42} &= -\frac{m_c x_2}{M^2}, & V_L^{43} &= -\frac{m_t}{M} \sin \theta_R, & V_L^{44} &= \frac{m_{t'}}{M} \cos \theta_R; \end{aligned} \quad (2.7)$$

while the remaining terms can be found in [24]. The formulas show that the left-handed mixing with the light quarks, V_L^{41} and V_L^{42} , can be safely neglected being suppressed by the light quark masses. The matrices V_L and V_R will also introduce a flavour mixing in the up sector: the most dangerous effect is the presence of flavour changing couplings to the Z boson, due to the fact that the couplings of U to the Z differ from the couplings of the SM up quarks. The down quark sector is not directly affected by the presence of the vector-like doublet, thus the precise measurements in the Kaon and B meson sector do not pose tight bounds in our case. The tree level FCNCs generated by the Z couplings also depend on the same matrix elements appearing in the $X_{5/3}$ couplings, thus we can derive bounds on the couplings from flavour observables. The most severe bounds come from the D mesons, in particular from $D_0-\bar{D}_0$ mixing which is the most stringent bound on flavour violation for this non-standard doublet case. In particular the most important constraint are on the right mixing matrix V_R . A summary of the relevant bounds on the mixing with the up $|V_R^{41}|$ and down $|V_R^{42}|$ can be found in [24] and is summarised in Table 1. The bound on rare top decays has been updated with respect to the one quoted in [24]: CMS has undertaken a study of rare top decay with an integrated luminosity of 5 fb^{-1}

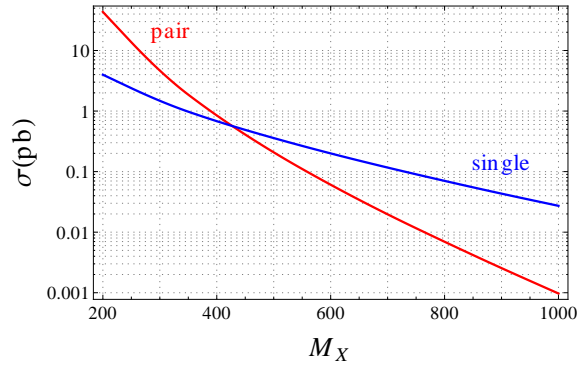


Figure 1. Production cross-sections of $X_{5/3}$ as function of the mass M_X . In blue the single production cross-section $pp \rightarrow X_{5/3} + Y$, where $Y = W^\pm$ or a light quark; in red the pair production contribution $pp \rightarrow X_{5/3} \bar{X}_{5/3}$. The mixing parameters, which determine the single production, are $\sin \theta_R = 0.3$, $V_R^{42} = 0.2$, $V_R^{41} = 3.2 \times 10^{-4}/V_R^{42} = 1.6 \times 10^{-3}$.

[26], finding a limit $\Gamma(t \rightarrow Zq)/\Gamma(t \rightarrow Wb) < 0.24\%$. The strong limit from D_0 – \bar{D}_0 mixing is on the product of the mixing with the first and second generation, while the bounds on the individual mixing terms are rather mild, coming from Atomic Parity Violation (APV) experiments for the up and from LEP1 measurements of the charm couplings to the Z boson. While respecting the other bounds given in Table 1, either one of the two mixings can be fairly large, thus giving significant branching ratios of $X_{5/3}$ into Wc and Wu . The branching depends on the mixing with the top, which is bound from electroweak precision measurements (T parameter): the precise bound is mass dependent, however it is typically of the order $|V_R^{43}| = \sin \theta_R < 0.3$. In the following section we further discuss this point.

2.1 $X_{5/3}$ production and decay

The $X_{5/3}$ vector-like quark can be both single and pair produced. Pair production is dominated by QCD processes from gluon pairs and quark pairs. At LHC energies the production from gluons is dominant. The corresponding couplings are model independent as only dictated by the colour quantum numbers. Electroweak diagrams are sub-dominant, coming from quark pairs into gauge bosons. Single production is more model dependent because it occurs via quark pairs going into $X_{5/3}$ and standard quarks through the exchange of a W boson. One can note that pair production, being mainly of QCD origin is dominant at low masses of the $X_{5/3}$ vector-like quark but decreases faster than single production when the mass of the $X_{5/3}$ quark increases. This is a well-known behaviour, which is due to the decrease of the parton distribution functions with the centre of mass energy of the parton-level collision. The detailed behaviour as a function of the $X_{5/3}$ quark mass is given in Figure 1 for a specific choice of the mixing parameters. The $X_{5/3}$ vector-like quark can decay into up-type quarks ($X_{5/3} \rightarrow W^+ u_i$) but not into $W^+ t'$ for the following reasons:

- if the $X_{5/3}$ and t' are lighter than the top quark, the mass gap between $X_{5/3}$ and t' is too small. This case is nevertheless disfavoured by present bounds on new heavy states;

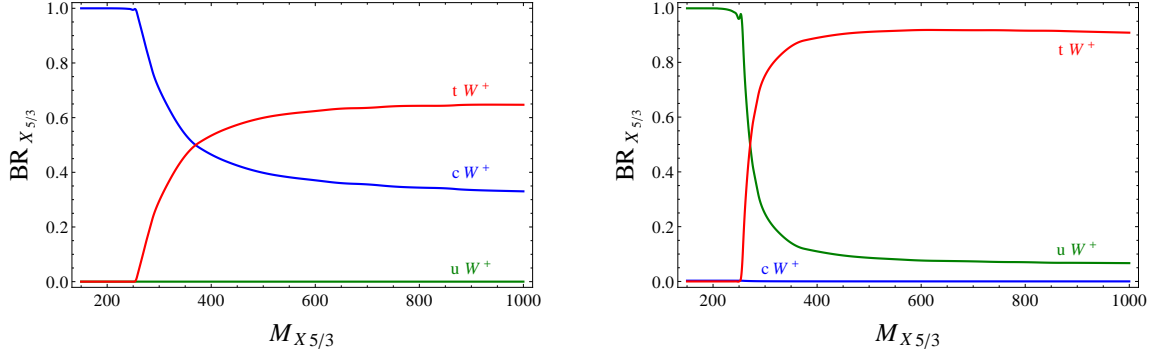


Figure 2. Branching ratios of $X_{5/3}$ as function of $X_{5/3}$ mass. In the left panel the mixing parameters are $\sin \theta_R = 0.3$, $V_R^{42} = 0.2$, $V_R^{41} = 3.2 \times 10^{-4}/V_R^{42}$. This particular choice maximises V_R^{42} . In the right panel the mixing parameters are $\sin \theta_R = 0.3$, $V_R^{41} = 0.078$, $V_R^{42} = 3.2 \times 10^{-4}/V_R^{41}$. This particular choice maximises V_R^{41} .

- if the $X_{5/3}$ and t' are heavier than the top quark, the mass hierarchy is $M_X < m_{t'}$, as explained in the previous section.

The branching ratios for parameters saturating the flavour bounds and for fixed $\sin \theta_R = 0.3$, are shown in Figure 2. It is possible to see that choosing to maximise the mixing with the charm, $|V_R^{42}|$, the decay into Wu is negligible: this is due to the constraint on the product of mixing parameters coming from the $D_0 - \bar{D}_0$ mixing. On the other hand, choosing to maximise the mixing with the up, $|V_R^{41}|$, the situation would be reversed, with the decay into Wc being irrelevant. The plots show in both cases sizeable decay rates into light quarks: this rate can be further enhanced if one chooses smaller mixing with the top, and can be 100% in the extreme limit $\sin \theta_R = 0$. As this possibility is not excluded, the branching into light quarks is virtually a free parameter. The single production cross section, on the other hand, is proportional to the mixing parameters and therefore is crucially dependent on how large V_R^{42} and V_R^{41} are, while the production cross section for the $X_{5/3}$ pair is in practice insensitive to the particular choice of mixing in the light sector. To summarize, when considering QCD pair production, the only dependence on the specific vector-like representation is encoded in the branching ratios, but this dependence can be completely removed if experimental efficiencies in the different channels were known. The phenomenology of different scenarios could then be described by simple rescalings of experimental data. In the following we choose a benchmark point that maximises $|V_R^{42}|$: in this case the branching ratio to Wt is more suppressed, representing a scenario which is different from the one commonly searched in experimental analyses. We will then generalise our results in Section 4.2, allowing the branching ratio to Wt to be a free parameter, in order to cover all possible parameter ranges and to allow a comparison to published experimental searches with $BR(X_{5/3} \rightarrow Wt) = 100\%$.

2.2 Present bounds

In this section bounds coming from direct searches of heavy fermions at the LHC will be summarised. The most stringent direct bounds on the mass of the $X_{5/3}$ come from very

recent searches for pair production of $X_{5/3}$ decaying 100% into Wt in both ATLAS and CMS experiments. However, processes involving down-type quarks decaying via $b' \rightarrow Wt$, as the pair production $b'\bar{b}' \rightarrow W^-tW^+\bar{t}$, have the same final state as the pair production of $X_{5/3}$ which decays 100% to top quark and W boson: $X_{5/3}\bar{X}_{5/3} \rightarrow W^+tW^-\bar{t}$, the only difference being that the charges of the two W s are flipped. Therefore, bounds coming from searches of pair production of $b' \rightarrow W^-t$ can be directly translated in bounds for $X_{5/3} \rightarrow W^+t$.

The strongest bounds from ATLAS have been obtained in [27], with a sample corresponding to an integrated luminosity of 4.7fb^{-1} : considering $X_{5/3}$ pair production and looking for a same-sign dilepton channel, the bound on the $X_{5/3}$ mass obtained by this search is $M_X > 670$ GeV; the same search includes also the contribution of single $X_{5/3}$ production under various assumptions on its coupling with Wt , and the obtained bound raises to $680 - 700$ GeV. In [28], corresponding to an integrated luminosity of 4.64fb^{-1} , the single production of heavy quarks decaying only to light generations is studied: the quoted bound for $X_{5/3}$ is $m_X > 1420$ GeV, but since it relies on specific assumptions on the coupling between $X_{5/3}$ and light generations, it will not be considered in this study. ATLAS has also performed two analyses for a b' using 1.04fb^{-1} [22, 29] finding that at 95% confidence level a b' quark with mass $m'_b < 480$ GeV decaying entirely via $b' \rightarrow Wt$ is excluded.

In CMS, the strongest bounds have been obtained in [17] and [30]. The first search has been performed in the same-sign dilepton channel using a data sample corresponding to an integrated luminosity of 5fb^{-1} , and the bound on the mass of $X_{5/3}$ obtained from that analysis is $M_X > 645$ GeV. Since this search has been used to validate our analysis, more details will be illustrated in the following section. The second search [30] was performed for a quark Q , pair produced by the strong interactions and decaying exclusively into a top quark and a W or Z boson. For a down type quark decaying 100% into Wt , a mass below 675 GeV is excluded at the 95% of confidence level. Previous direct bounds from CMS [21] on b' quarks obtained $m'_b < 611$ GeV excluded at 95% confidence level assuming 100% decay to top quark and W boson.

Note however that all these high mass bounds rely on the strong and unrealistic assumption that only one decay channel is present. In more realistic scenarios the $X_{5/3}$ quark can have sizeable decay modes to lighter quarks.

Searches of t' with mixing only to third generation can also provide bounds for $X_{5/3}$ in our specific model, since $m_{t'}$ is related to $M_X (= M)$ and to mixing parameters through the relation in Eq. (2.5).

The strongest bounds on t' by the ATLAS collaboration have been obtained in [31], using a sample of 4.7fb^{-1} and considering a lepton+jets final state: in this study the t' is supposed either to decay 100% to Wb or to decay both through charged and neutral currents to Wb, Zt and Ht . Two bounds are therefore provided: if the t' can only decay to Wb it must be heavier than 656 GeV at 95% C.L., while considering the more realistic scenarios with $BR(tW) = 50\%$ and $BR(Ht) = BR(Zt) = 33\%$, the bound is rescaled to 500 GeV. This search clearly shows how the bounds can be overestimated if considering just one decay channel. In the single production search [28] described above, the bound

for t' decaying 100% to Zq is 1080 GeV, but as already stated, this bound will not be considered as it relies on specific assumptions.

CMS has searched for a t' which mixes with third generation. In [32], a search for pair production of t' with $BR(Wb)=100\%$ has been undertaken in the leptons+jet channel with a sample of 5fb^{-1} , finding the 95% C.L. bound $m_{t'} > 560$ GeV; a similar search [33] at the same integrated luminosity obtains a nearly identical bound, 557 GeV. In [34], using a sample of 1.14fb^{-1} , a search for pair production of t' assumed to decay 100% into tZ gives a bound on t' with mass $m_{t'} > 475$ GeV at 95% confidence level.

3 Simulation Details

Our study is performed for the LHC at 7 TeV in the centre of mass, assuming a luminosity of 5fb^{-1} . The analysis is performed using **MadGraph5** [35] for generating the signal. Matching to **Pythia** [36] is used for the hadronisation process, and a simplified detector simulation using **Delphes** [37] to match the signal with the CMS experimental set up. We chose the CMS set-up in order to validate our simulation with the published search in [17], and to be able to compare our results.

3.1 Signal

The signal consists of inclusive pair production of $X_{5/3}$ plus QCD radiation and is given by the following process:

$$pp \rightarrow X_{5/3} \bar{X}_{5/3} (+Y) + (n \leq 2) \text{ jets} \quad (3.1)$$

where $Y = W^\pm, Z, \gamma$ and the b-jets are included in the QCD radiation. Processes with additional electroweak gauge bosons in the final state are always suppressed by phase space and weak couplings (with the exception of $Y = \gamma$), but they have been kept nevertheless because they provide a source of leptons in the final state. The channels with $Y = t, t', h$ have a negligible cross section and will be ignored in the following analysis. The relative contributions of the different channels with the kinematic cuts described below and for different $X_{5/3}$ masses are shown in Table 2. We have quoted both LO and NLO+NNLL cross sections. The LO cross sections are those resulting from MadGraph before applying the matching procedure and are shown for reference purposes, while the NLO+NNLL cross sections, used to compare our results to CMS analyses, have been taken from Ref.[38]. Note indeed that, after the matching, the contributions of the various sub-processes are distributed differently as they contain modified contributions from processes with jets. The $X_{5/3}$ quark is always considered on-shell and it subsequently decays to Wu_i with branching ratios which depend on the $X_{5/3}$ mass (see Figure 2). We have performed a scan over the $X_{5/3}$ mass in the range $\{300, 700\}$ GeV with steps of 100 GeV. Below the $M_X = m_W + m_t \sim 250$ GeV limit the decay into Wt would not be allowed, strongly reducing same sign dilepton events in the final state.

The matching procedure has been performed following the k_T -MLM scheme, automatically implemented in **Madgraph5+Pythia**, and the matching parameter **xqcut** implemented

M_X (GeV)	cross sections [pb]			BR(Wt) %	Expected events with $\ell^\pm\ell^\pm$ %
	LO $X_{5/3}\bar{X}_{5/3}$	$X_{5/3}\bar{X}_{5/3} + Y$	NLO + NNLL $X_{5/3}\bar{X}_{5/3}$		
300	4.625	0.184	7.826	29.5	3.7
400	0.847	0.032	1.379	53.4	6.7
500	0.207	0.009	0.324	59.9	7.5
600	0.061	0.003	0.091	62.4	7.8
700	0.020	0.001	0.029	63.6	8.0

Table 2. Weights of different signal channels. Branching ratio of $X_{5/3} \rightarrow Wt$ and expected rate of signal events with a pair of same sign leptons as function of the $X_{5/3}$ mass.

in `Madgraph5` has been computed in every step of the scan to optimise the matching procedure for each $X_{5/3}$ mass value.

3.2 Identification of SM backgrounds

Reconstructing the $X_{5/3}$ quarks individually is a very difficult task, which suffers from huge combinatorial background. In addition, in the complex environment of the LHC, final state objects overlap and their individual reconstruction is not efficient. In order to get rid of the huge multi-jet background, we study the potential of a same sign dilepton signature. Depending on the $X_{5/3}$ mass and for our choice of parameters, this signal varies roughly from 2% to 4% of the total cross section (see Table 2).

In the following we consider only electrons and muons. There are two main categories of backgrounds: one is represented by $t\bar{t}$ +jets, Vqq (where $V=W$ or Z) and Z +jets. They do not contain opposite sign dileptons, but their cross-section is large enough to fake a same sign dilepton signature because of the charge misidentification of the leptons. The second category of background is the one with two real same sign dileptons. We have considered VV +jets, $Zt\bar{t}$ +jets and $Wt\bar{t}$ +jets. The cross sections of the aforementioned processes are smaller, but they yield an irreducible background. All these backgrounds and their cross-sections are summarised in Table 3. Due to the recent discovery of a Higgs-like state at the LHC, we have also estimated the contribution of the $t\bar{t}H$ background, which falls within either the first or the second category depending on the decay channel of the Higgs boson. Assuming a Higgs mass of 125 GeV we have found that this background can be safely neglected, as will be shown in Section 4.1.

3.3 Detector simulation

As explained before, background and signal events are generated with `MadGraph/MadEvent`. In order to take into account the efficiency of event selection under semi-realistic experimental conditions, the detector simulation is carried out with the fast detector simulator `Delphes` [37] using the CMS detector model. The tracker is assumed to reconstruct tracks within $|\eta| < 2.4$ with a 100% efficiency and the calorimeters cover a pseudo-rapidity region up to $|\eta| < 3$ with an electromagnetic and hadronic tower segmentation corresponding to

Background process	cross-section [pb]
Z +jets	2800
$t\bar{t}$ +jets	165
Vqq	36
VV +jets	5
$Wt\bar{t}$	0.169
$Zt\bar{t}$	0.139

Table 3. List of backgrounds considered in this analysis. The cross sections for all processes are at the LO, as obtained from the `MadEvent` calculator [39], except for $t\bar{t}$ events for which the approximate NLO calculation of [40] is used.

object	$ \eta_{max} $	p_T^{min} [GeV]
e, μ	2.4	10
jets	3	20
b-jets	2.5	20

Table 4. Acceptance criteria of the various final states in the simulated detector.

the CMS detector. The energy of each quasi stable particle is summed up in the corresponding calorimeter tower. The resulting energy is then smeared according to resolution functions assigned to the electromagnetic calorimeter (EC) and the hadronic calorimeter (HC). The acceptance criteria are summarised in Table 4. For the leptons (electrons and muons), we require a tight isolation criterion: no additional tracks with $p_T > 2$ GeV must be present in a cone $\Delta R = \sqrt{\Delta\eta^2 + \Delta\phi^2} = 0.5$ centred on the lepton track. The jets are reconstructed using only the calorimeter towers, through the anti-kt algorithm with cone size radius of 0.5, as defined in the `FastJet` package [41] and implemented in `Delphes`. The b-tagging efficiency is assumed to be 40% for all b-jets, independently of their transverse momentum, with a fake rate of 1% (10%) for light (charm) jets. Finally, the total missing transverse energy (MET) is reconstructed using information from the calorimetric towers and muon candidates only.

In the following, we present a simple strategy that can lead to promising Signal-over-Background (S/B) ratios. Our purpose is to illustrate the new possibilities that open up in the $X_{5/3} \bar{X}_{5/3}$ final state and motivate more detailed studies. To this aim detailed information on the efficiencies and the visible cross sections are given.

4 Analysis and results

As outlined before, we request two isolated same sign leptons in the final state. Two well reconstructed leptons with $p_T > 30$ GeV and $|\eta| < 2.4$ are sufficient to trigger the events (the two lepton combined trigger efficiency is assumed to be 100% after the lepton selection cut). Selected jets have $p_T > 30$ GeV and $|\eta| < 2.5$.

The distributions of the number of jets and HT (which is defined as the scalar sum of all the selected jets in the event) after the various steps of the selection are shown on Figure 3 where for the signal the mass is 600 GeV/ c^2 . After requesting two same sign isolated leptons, the dominant background contributions are VV +jets and $t\bar{t}$. VV +jets can produce two real isolated leptons but signal and background are well separated both in the number of hard jets and HT. The $t\bar{t}$ contribution fulfils the two same sign isolated requirement when one lepton inside a b-jet can be seen as isolated. In order to help to remove this contribution, a cut on the angular distance between the lepton and the closest jet, $\Delta R_{min}(\ell, \text{jet})$, is used. The final selection, shown in the last row of Figure 3, consists of two same sign isolated leptons, $HT \geq 200$ GeV, at least two jets and $\Delta R_{min}(\ell, \text{jet}) > 0.5$. This selection removes most of the background and retains roughly all the signal events. For $M_X=600$ GeV/ c^2 and an integrated luminosity of 5 fb $^{-1}$, the signal over background ratio is $3 \cdot 10^{-5}$ without selection, with the requirement of two same sign leptons it rises at 0.05, and it is of the order of 1 for the final selection. Because it has been obtained using a fast detector simulation and to be distinguished from what is used in CMS, this selection will be referred to as *fast selection* in the following.

4.1 Mass limit for fixed BRs

The number of background (B) and signal (S) events surviving the final selection, is evaluated assuming an integrated luminosity of 5 fb $^{-1}$. The significance of an eventual signal is computed as S/\sqrt{B} . Table 5 and Figures 4 and 5 show the evolution of the significance as a function of the mass. In Table 5 we also reported the efficiency on the inclusive signal after the same sign selection and after the final selection: the two numbers are quite close, thus showing that the additional cuts on H_T and on the number of jets do not significantly affect the signal yield. For the $t\bar{t}H$ background we have used the cross section and branching ratios provided by the LHC Higgs Cross Section Working Group [42]: considering a cross section at 7 TeV of 0.0863 pb, corresponding to a Higgs mass of 125 GeV, we have obtained a contribution to the background yield of (0.47 ± 0.45) , which is negligible with respect to the rest of the backgrounds and therefore will not be considered in the following analysis. This selection would allow an observation of a signal with a mass ranging from the tW production threshold up to 561 GeV and an evidence up to 609 GeV. These limits are valid assuming that the $BR(X \rightarrow Wt)$ is fixed to a value depending on M_X in the specific model (the corresponding values are given in Table 2). Searches of this kind have been performed with LHC data. To compare with the actual available results, we reproduce the selection made in the CMS search [17]. This selection requires two well reconstructed leptons with $p_T > 30$ GeV, at least four jets with $p_T > 30$ GeV and $|\eta| < 2.5$, $H_T > 300$. The selection also includes a veto of the region around the Z mass peak. We use this alternative selection (which will be referred to as *CMS selection* in the following) as a reference. Since we are using a fast simulation, reproducing the reliability of the CMS study is behind our scope, nevertheless we want to check that we are able to reproduce reasonably the performances detailed in [17]. Since the study presented in [17] only considers the case in which $BR(X \rightarrow Wt) = 1$, we restrict our study to such events in order

Mass (GeV)	Signal yield	Background yield	S/\sqrt{B}	Efficiency final	Efficiency same sign
300	262.6 ± 17.3	12.5 ± 1.66	74.3 ± 6.9	$(0.67 \pm 0.04)\%$	$(1.07 \pm 0.055)\%$
400	119.1 ± 4.9	12.5 ± 1.66	33.7 ± 2.6	$(1.73 \pm 0.07)\%$	$(2.28 \pm 0.08)\%$
500	36.2 ± 1.3	12.5 ± 1.66	10.2 ± 0.8	$(2.24 \pm 0.08)\%$	$(2.86 \pm 0.09)\%$
600	10.7 ± 0.3	12.5 ± 1.66	3.0 ± 0.2	$(2.36 \pm 0.08)\%$	$(3.08 \pm 0.09)\%$
700	4.1 ± 0.2	12.5 ± 1.66	1.2 ± 0.1	$(2.84 \pm 0.09)\%$	$(3.52 \pm 0.095)\%$

Table 5. Background and signal event yields for an integrated luminosity of 5 fb^{-1} , after the final selection. The S/\sqrt{B} ratios is also provided. In the right-columns we also reported the inclusive efficiency after the final selection and after the same-sign dilepton selection.

Mass (GeV)	Final selection		Same-sign selection	
	$\epsilon (\text{WtWt})$	$\epsilon (\text{WtWc})$	$\epsilon (\text{WtWt})$	$\epsilon (\text{WtWc})$
300	$(2.1 \pm 0.3)\%$	$(1.2 \pm 0.1)\%$	$(3.7 \pm 0.3)\%$	$(1.8 \pm 0.1)\%$
400	$(3.0 \pm 0.2)\%$	$(1.7 \pm 0.1)\%$	$(4.1 \pm 0.2)\%$	$(2.3 \pm 0.1)\%$
500	$(3.7 \pm 0.2)\%$	$(1.9 \pm 0.1)\%$	$(4.8 \pm 0.2)\%$	$(2.4 \pm 0.1)\%$
600	$(3.7 \pm 0.2)\%$	$(1.9 \pm 0.1)\%$	$(4.8 \pm 0.2)\%$	$(2.6 \pm 0.1)\%$
700	$(4.2 \pm 0.2)\%$	$(2.4 \pm 0.1)\%$	$(5.4 \pm 0.2)\%$	$(2.9 \pm 0.1)\%$

Table 6. Signal selection efficiencies for different masses listed separately for events in which both $X_{5/3}$ decay via the Wt channel and events in which one $X_{5/3}$ decays to Wt and the other to Wc. In both cases, the efficiencies are calculated on the inclusive samples and not restricted to the same sign leptons sub-sample. For comparison, we also list the efficiencies after the same-sign selection.

to compare. The performance of such a selection on simulated signal events is found to be roughly comparable with the one described in [17].

The significance of an eventual signal as a function of the signal generated mass, is shown in Figure 4 for the two selections, in the hypothesis of $BR(X \rightarrow Wt) = 1$ (left plot). In this case the fast selection would allow an observation of a signal with a mass ranging from the tW production threshold up to 603 GeV and an evidence up to 653 GeV (when emulating the CMS selection, the corresponding values are 609 and 653 GeV). In the right plot in Figure 4 we also show the significance of the signal if only the mixed decayed events are considered. The signal selection efficiencies for different masses are listed in Table 6, separately for events in which both $X_{5/3}$ decay via the Wt channel (left) and events in which one $X_{5/3}$ decays to Wt and the other to Wc (right). As the listed numbers include the effect of the W boson branching ratio into leptons, in the case of equal efficiencies of the cuts, the efficiencies in the two channels should be $\epsilon (\text{WtWt}) = 2 \times \epsilon (\text{WtWc})$: the numbers in the table, therefore, show that the *fast selection* is more efficient on the mixed decay sample than in the 100% Wt sample.

The same study has been repeated on signal samples for which the value of $BR(X \rightarrow Wt)$ is fixed to a value depending on M_X (according to Table 2), and hence composed of

both events with both $X_{5/3}$ decay via the Wt channel and events in which one $X_{5/3}$ decays to Wt and the other one to Wc (the events where both $X_{5/3}$ decay via the Wc channel are not surviving the request of two same sign leptons). The CMS selection being tuned under the assumption of $BR(X \rightarrow Wt) = 1$, it is less optimal when one of the $X_{5/3}$ decays to Wc , while the fast selection, tuned on a sample with $BR(X \rightarrow Wt) \neq 1$ (see exact values in Table 2) has better performances. As an example, the different cut on the number of jets in the event can have an impact, as can be seen in Figure 6, where the distribution of the number of jets is shown after requesting two same sign leptons and after the final fast selection, separately for signal event where both $X_{5/3}$ decay in the Wt channel, and in the case where one $X_{5/3}$ decays to Wt and the other to Wc . This comparison shows that considering the more general case $BR(X \rightarrow Wt) \neq 1$ may lead to improved efficiency in the search for $X_{5/3}$ states.

The reach of this analysis is further enhanced in the recent data collected by the LHC at 8TeV. From a rough evaluation using the efficiencies obtained in the present study, taking into account the increase in cross sections (for both signal and background processes), and assuming an integrated luminosity of 19/fb (corresponding to the data collected by CMS at 8TeV in 2012), we expect the significance to increase by a factor of 2.5–3 for the different mass points considered. This selection would thus allow to raise the bound on $X_{5/3}$ mass to above 700 GeV for having an evidence of the signal.

4.2 Analysis with $BR(X_{5/3} \rightarrow tW)$ as a free parameter

In the previous sections, the magnitude of the decay rate of $X_{5/3}$ to Wt , $BR(X \rightarrow Wt)$ was chosen depending on the value of M_X (see Table 2). In order to have an idea of the possible reach and limits without imposing a specific link between mass and branching ratios, in this section we let the decay rate free to vary between 0 and 1. We study the significance of such a signal as a function of the decay rate. The study is performed separately and independently for each mass point, and we assume $BR(X \rightarrow Wt) = 1 - BR(X \rightarrow Wc)$ (that is V_R^{42} maximal; we discussed in Sect. 2.1 that the particular choice of mixing in the light sector does not change significantly the production cross section). Figure 7 shows the significance S/\sqrt{B} as a function of $BR(X \rightarrow Wt)$ for different M_X values. As expected the significance increases with $BR(X \rightarrow Wt)$. For masses above 600 GeV/c², it is not possible to obtain an evidence of the signal with an integrated luminosity of 5/fb. In the right panel of Figure 7 we also show the needed luminosity for a 5 σ significance as a function of $BR(X \rightarrow Wt)$ for different M_X values. For a mass of 600 GeV/c², an integrated luminosity of 6/fb is needed in the best case scenario. In Figure 8, the evolution of the significance with the value of $BR(X \rightarrow Wt)$ is shown for the fast selection, compared to the reference CMS selection. The plot shows that significant improvements may be achieved for comparable decay rates into tops and light quarks. The results of this study are only qualitative, as a more realistic simulation of the detector performance and optimisation of the cut for various masses would be required to validate it.

5 Conclusions

The search for a vector-like quark $X_{5/3}$ gives important bounds on the structure of possible extensions of the SM. In this paper we have used the requirement for two isolated leptons of the same sign to analyse the signal coming from pair production of the exotic $X_{5/3}$ vector-like quark at LHC. We have performed a detailed analysis using a Monte Carlo simulation taking into account both signal and background and a simplified detector simulation to have a more detailed idea of the perspectives for detection or exclusion for the LHC experiments. The novelty of our study is that we consider the most general scenario, where the exotic $X_{5/3}$ quark is allowed to decay both into W^+t and in light quarks, W^+c and W^+u . We point out that the channel with one $X_{5/3}$ decaying into a top and the other into a light quark will also contribute to the same sign dilepton signal, and that it is crucial to know the efficiency of the experimental search on this channel, together with the W^+tW^-t in order to extract a realistic bound on the $X_{5/3}$ mass. We also point out the possible relevance of single $X_{5/3}$ production.

After validating our simulation with the dedicated CMS search, where 100% decays into tops are assumed, we propose a different set of cuts, with a lower cut in H_T , a minimal cut in the number of jets and using the lepton isolation as the main cut to reduce the $t\bar{t}$ background. Our results show that the two sets of cuts give similar significance S/\sqrt{B} in the 100% $X_{5/3} \rightarrow W^+t$ case, while our selection offers a better efficiency in the mixed case. In the case of large rate into light quarks, the same sign dilepton strategy is complemented by the CMS search where heavy quarks decaying into W plus light jets are fully reconstructed. While we do not advocate our selection cuts as being optimal, the results of our study motivate a more detailed study of the LHC discovery potential of a vector-like quark with charge $+5/3$, beyond the approximation of 100% decays into tops.

Acknowledgements

This project was partially supported by a “Theory LHC France 2012” grant from IN2P3. We also acknowledge the warm hospitality of the CMS centre in Lyon for discussions.

References

- [1] M. Schmaltz and D. Tucker-Smith, Ann. Rev. Nucl. Part. Sci. **55** (2005) 229 [[arXiv:hep-ph/0502182](#)].
- [2] K. Agashe, R. Contino and A. Pomarol, Nucl. Phys. B **719** (2005) 165 [[arXiv:hep-ph/0412089](#)];
- [3] K. Agashe, R. Contino, L. Da Rold and A. Pomarol, Phys. Lett. B **641** (2006) 62 [[hep-ph/0605341](#)].
- [4] T. Moroi and Y. Okada, Mod. Phys. Lett. A **7** (1992) 187.
- [5] S. P. Martin, Phys. Rev. D **81** (2010) 035004 [[arXiv:0910.2732](#) [hep-ph]].
- [6] P. W. Graham, A. Ismail, S. Rajendran and P. Saraswat, Phys. Rev. D **81** (2010) 055016 [[arXiv:0910.3020](#) [hep-ph]].

- [7] A. Azatov, O. Bondu, A. Falkowski, M. Felcini, S. Gascon-Shotkin, D. K. Ghosh, G. Moreau and S. Sekmen, Phys. Rev. D **85** (2012) 115022 [[arXiv:1204.0455](#) [hep-ph]].
- [8] N. Bonne and G. Moreau, Phys. Lett. B **717** (2012) 409 [[arXiv:1206.3360](#) [hep-ph]].
- [9] G. Moreau, [[arXiv:1210.3977](#) [hep-ph]].
- [10] G. Cacciapaglia, A. Deandrea and J. Llodra-Perez, JHEP **0906** (2009) 054 [[arXiv:0901.0927](#) [hep-ph]].
- [11] G. Cacciapaglia, A. Deandrea, G. Drieu La Rochelle and J. -B. Flament, [[arXiv:1210.8120](#) [hep-ph]].
- [12] G. Cacciapaglia, A. Deandrea, D. Harada and Y. Okada, JHEP **1011** (2010) 159 [[arXiv:1007.2933](#) [hep-ph]].
- [13] J. Alwall *et al.*, Eur. Phys. J. C **49** (2007) 791 [[arXiv:hep-ph/0607115](#)].
- [14] F. del Aguila *et al.*, Eur. Phys. J. C **57** (2008) 183 [[arXiv:0801.1800](#) [hep-ph]].
- [15] Y. Okada and L. Panizzi, [[arXiv:1207.5607](#) [hep-ph]].
- [16] J. A. Aguilar-Saavedra, JHEP **0911** (2009) 030 [[arXiv:0907.3155](#) [hep-ph]].
- [17] [CMS Collaboration], [CMS-PAS-B2G-12-003](#).
- [18] R. Contino and G. Servant, JHEP **0806** (2008) 026 [[arXiv:0801.1679](#) [hep-ph]].
- [19] J. Mrazek and A. Wulzer, Phys. Rev. D **81** (2010) 075006 [[arXiv:0909.3977](#) [hep-ph]].
- [20] G. Dissertori, E. Furlan, F. Moortgat and P. Nef, JHEP **1009** (2010) 019 [[arXiv:1005.4414](#) [hep-ph]].
- [21] S. Chatrchyan *et al.* [CMS Collaboration], JHEP **1205** (2012) 123 [[arXiv:1204.1088](#) [hep-ex]].
- [22] G. Aad *et al.* [ATLAS Collaboration], JHEP **1204** (2012) 069 [[arXiv:1202.5520](#) [hep-ex]].
- [23] O. Matsedonskyi, G. Panico and A. Wulzer, [[arXiv:1204.6333](#) [hep-ph]].
- [24] G. Cacciapaglia, A. Deandrea, L. Panizzi, N. Gaur, D. Harada and Y. Okada, JHEP **1203** (2012) 070 [[arXiv:1108.6329](#) [hep-ph]].
- [25] G. Aad *et al.* [ATLAS Collaboration], Phys. Rev. D **86** (2012) 012007 [[arXiv:1202.3389](#) [hep-ex]].
- [26] S. Chatrchyan *et al.* [CMS Collaboration], [[arXiv:1208.0957](#) [hep-ex]].
- [27] [ATLAS Collaboration], [ATLAS-CONF-2012-130](#).
- [28] [ATLAS Collaboration], [ATLAS-CONF-2012-137](#).
- [29] G. Aad *et al.* [ATLAS Collaboration], Phys. Rev. Lett. **109** (2012) 032001 [[arXiv:1202.6540](#) [hep-ex]].
- [30] S. Chatrchyan *et al.* [CMS Collaboration], [[arXiv:1210.7471](#) [hep-ex]].
- [31] G. Aad *et al.* [ATLAS Collaboration], [[arXiv:1210.5468](#) [hep-ex]].
- [32] S. Chatrchyan *et al.* [CMS Collaboration], [[arXiv:1209.0471](#) [hep-ex]].
- [33] S. Chatrchyan *et al.* [CMS Collaboration], Phys. Lett. B **716** (2012) 103 [[arXiv:1203.5410](#) [hep-ex]].
- [34] S. Chatrchyan *et al.* [CMS Collaboration], Phys. Rev. Lett. **107** (2011) 271802 [[arXiv:1109.4985](#) [hep-ex]].

- [35] J. Alwall, M. Herquet, F. Maltoni, O. Mattelaer and T. Stelzer, JHEP **1106** (2011) 128 [[arXiv:1106.0522](#) [hep-ph]].
- [36] T. Sjostrand, S. Mrenna and P. Z. Skands, JHEP **0605** (2006) 026 [[hep-ph/0603175](#)].
- [37] S. Oryn, X. Rouby and V. Lemaitre, [[arXiv:0903.2225](#) [hep-ph]].
- [38] <http://www.lpthe.jussieu.fr/~cacciari/ttbar/>
- [39] J. Alwall, P. Demin, S. de Visscher, R. Frederix, M. Herquet, F. Maltoni, T. Plehn and D. L. Rainwater *et al.*, JHEP **0709** (2007) 028 [[arXiv:0706.2334](#) [hep-ph]].
- [40] N. Kidonakis, [[arXiv:0909.0037](#) [hep-ph]].
- [41] M. Cacciari, G. P. Salam and G. Soyez, Eur. Phys. J. C **72** (2012) 1896 [[arXiv:1111.6097](#) [hep-ph]].
- [42] <https://twiki.cern.ch/twiki/bin/view/LHCPhysics/CrossSections>

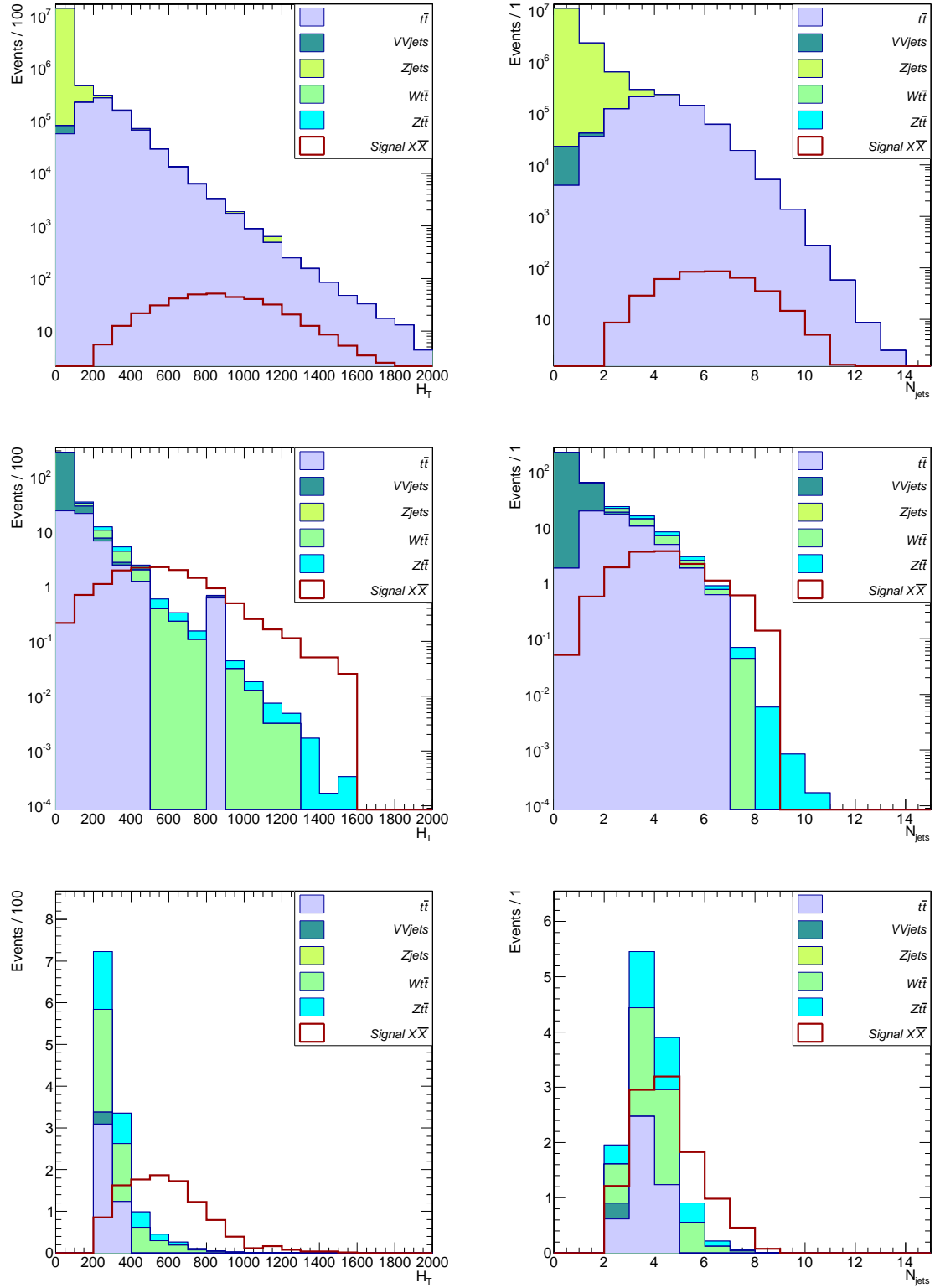


Figure 3. Number of expected events for a luminosity of 5fb^{-1} for the signal and SM backgrounds (stacked histogram) with respect to the number of jets (left) and HT (right). The first row shows the distributions without selection, the middle row after the requirement of two same sign leptons, and the last row when requesting two same sign leptons, a $\Delta R_{\min}(\ell, \text{jet}) > 0.5$ and at least two jets.

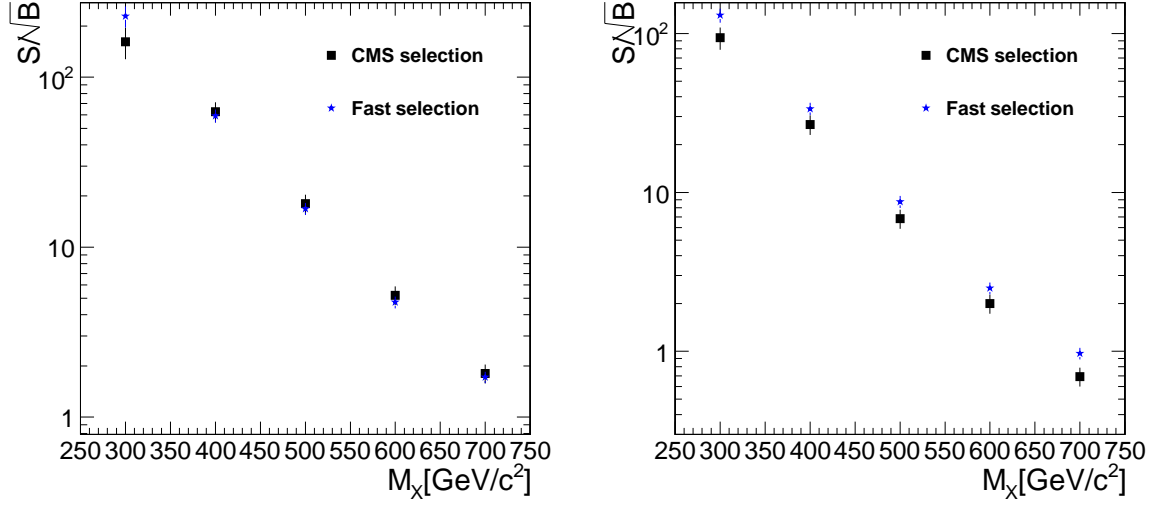


Figure 4. Significance of an eventual signal as a function of the signal generated mass, for fast and CMS selection, for events in which both $X_{5/3}$ decay via the Wt channel (left) and events in which one X decays to Wt and the other to Wc (right).

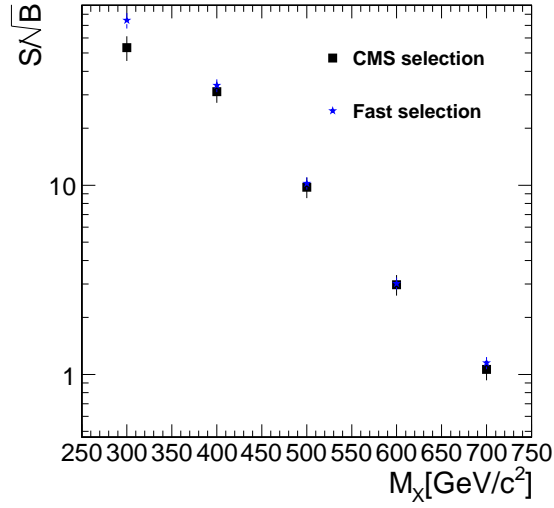


Figure 5. Significance of an eventual signal as a function of the signal generated mass, for fast and CMS selection, assuming $BR(X \rightarrow Wt)$ is fixed to a value depending on M_X .

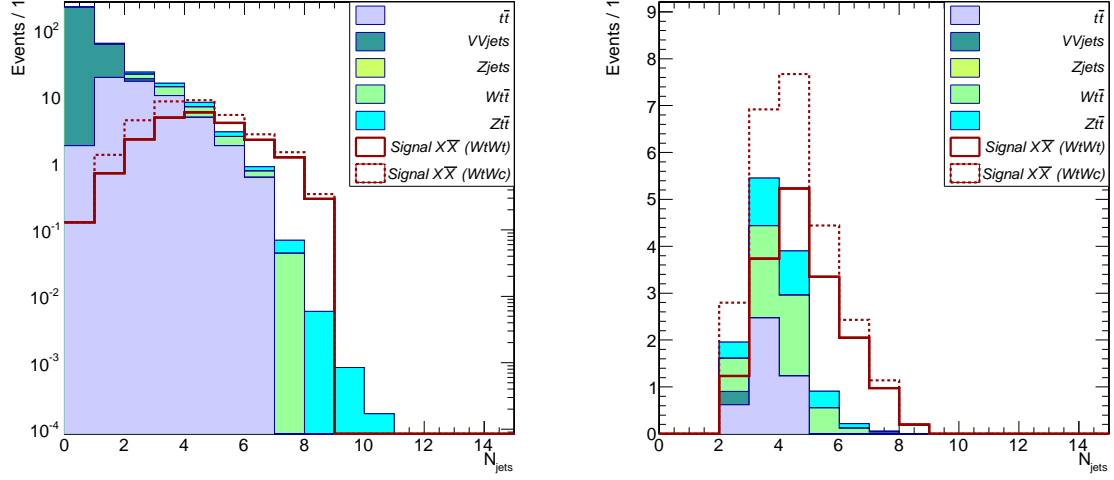


Figure 6. Number of expected events for a luminosity of 5fb^{-1} for the signal and SM backgrounds (stacked histogram) with respect to the number of good jets in the event. The left plot shows the distributions after the requirement of two same sign leptons, and the right one when requesting two same sign leptons, a $\Delta R_{\min}(\ell, \text{jet}) > 0.5$ and at least two jets.

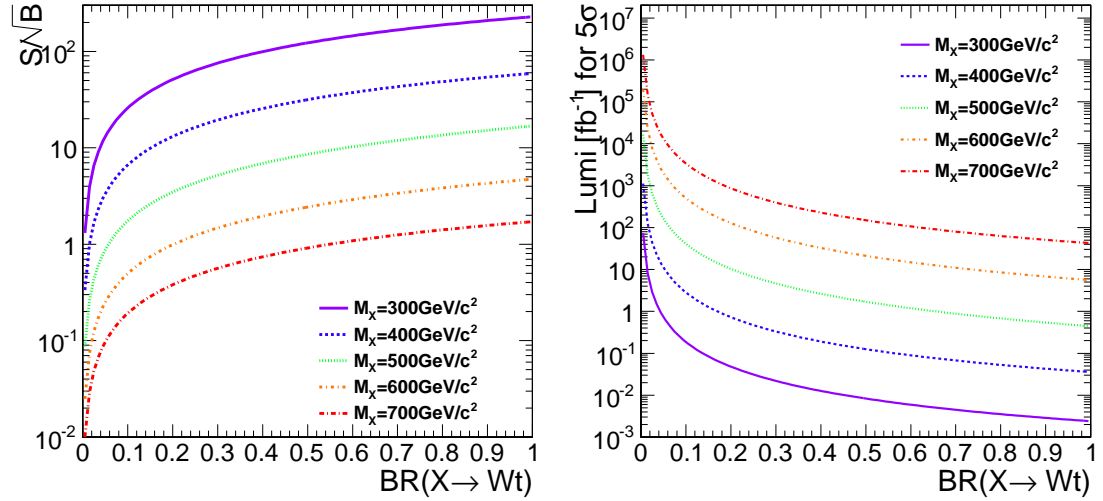


Figure 7. Significance for an integrated luminosity of $5/\text{fb}$ and luminosity needed for a 5σ significance as function of $BR(X \rightarrow Wt)$ for different M_X values.

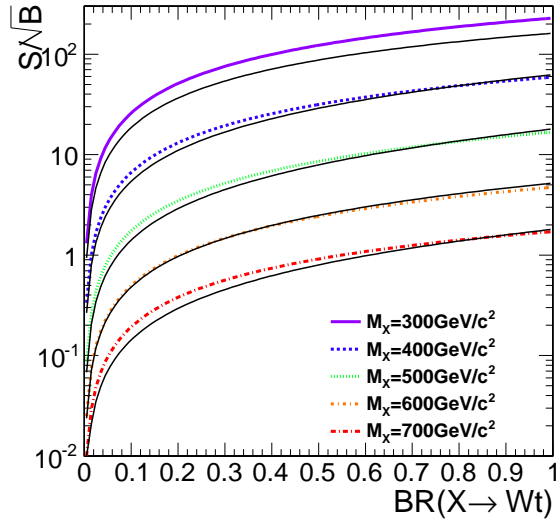


Figure 8. Significance as function of $BR(X \rightarrow Wt)$ for different M_X values for an integrated luminosity of 5/fb, compared for fast selection (coloured thick lines) and CMS selection (solid narrow lines).